



# Numerical investigation on thermal effects by adding thin compartmental plates into cooling enclosures with heat-leaking walls\*

Yong-hua HUANG<sup>†</sup>, Qiang CHEN

(Institute of Refrigeration and Cryogenics, Shanghai Jiao Tong University, Shanghai 200240, China)

<sup>†</sup>E-mail: huangyh@sjtu.edu.cn

Received Sept. 26, 2015; Revision accepted Apr. 13, 2016; Crosschecked May 11, 2016

**Abstract:** Adding thin compartmental plates near the internal walls of enclosures has been numerically modeled using the lattice Boltzmann method. This practice was found to be an effective way to further suppress the disadvantageous effects of heat leak, along with the application of insulation materials on the external surfaces. A modified extrapolation scheme for handling the thermal boundary of the thin plate was proposed and verified by comparison with the conventional coupled boundary scheme. The simulation of the natural convection during the cooling down processes and at steady states in the enclosure indicates that the existence of the plates leads to a higher cooling rate and a more favorable temperature uniformity. For a typical case, the one with plates takes 6% less time to reach the halfway point of the steady state and has 26% less temperature variance. Effects by the plates' positions and sizes were parametrically investigated, in order to find an optimal geometrical configuration. In addition, the fluid's intrinsic characteristics and the relative heat leak by using the Rayleigh number and Nusselt number, respectively, have been discussed in detail through hydrodynamic and convective heat transfer analyses.

**Key words:** Plate, Enclosure, Natural convection, Lattice Boltzmann, Cooling rate, Temperature uniformity  
<http://dx.doi.org/10.1631/jzus.A1500319>

**CLC number:** TB611

## 1 Introduction

Undesired heat exchange with the environment is a common problem in almost any kind of thermal system. For instance, heat leak is one of the major sources of thermal load for building design. In cryogenic applications, such as liquid hydrogen storage tanks, heat leak via radiation and structure conduction are the dominant causes for mass loss. To minimize the negative effects, wrapping insulating materials like polyurethane foam and installing a vacuum jacket on the external side of the objective body work as the most direct and effective approaches. It is certain that the effect of heat leak cannot be eliminated completely, as long as the temperature difference exists.

Nonetheless, it is possible to further reduce it by interrupting the heat transfer from the heat-leaking walls to the closed chamber's center area. In this study, we try to implement this idea by using a plate to alter the flow field near the walls, without introducing any additional heat source or sink. More specifically, such thin plates are mounted near but not contacting the heat-leaking walls, and not necessarily sealing off the near-wall space. It was found that such a setup provides a potential measure to further suppress heat leak in addition to the conventional insulations.

Natural convection driven by buoyancy in enclosures or cavities with plates has been extensively studied due to its wide thermal applications, such as the cooling of electronic components, heating and ventilation of building, and solar energy collectors. A large number of those studies treated the plate as either a heating or cooling source. Yang and Tao (1995) experimentally and numerically studied the natural convection in cubic enclosures with isolated

\* Project supported by the National Natural Science Foundation of China (No. 51176112)

ORCID: Yong-hua HUANG, <http://orcid.org/0000-0001-6453-8430>  
© Zhejiang University and Springer-Verlag Berlin Heidelberg 2016

heated or cooled plate suspended inside, where all the walls were maintained at a lower constant temperature. A following study with similar physical conditions on the transient process given by Ling *et al.* (1999) described a cubic enclosure with an internal vertical heating plate powered by a periodically varying input. Bilgen (2005) numerically studied the differentially heated cavity with a conductive fin (another form of plate) attached to the hot wall. The fin mainly serves as an extension of the hot wall; however, the effect on the heat transfer rate was mostly disadvantageous because of its greater influence on the flow field. Subsequently, Ben-Nakhi and Chamkha (2007) further considered an inclined thin fin with perfect conductivity, and presented discussions on parametric conditions. Altaç and Kurtul (2007) also investigated the effect of geometrical parameters on similar problems, but with an isolated hot plate, and proposed a correlation for the Nusselt number. Frederick (2007) studied a 3D cubical enclosure with a thick partition attached to the hot wall. Flow restrictions by the partition were found to be significant only at low Rayleigh numbers. Corvaro and Paroncini (2009) conducted experiments in the case where a heated strip was placed at the bottom center of an enclosure with colder walls. The “plate” mentioned under this context is generally referred to as one with certain considerable thickness compared with the dimensions of the enclosure.

Despite the relative richness of studies on the natural convection of enclosure with a plate inside, only a few of them considered the plate simply as a barrier to the flow field without bringing additional heat source and heat capacity. Jami *et al.* (2006) numerically calculated an inclined enclosure with a partition attached to one of the walls. The partition was a very thin plate and thermally penetrable. Costa (2012) numerically studied the natural convection in an enclosure with two partitions of finite thickness, regarding the influence by position, length, and thermal conductivity of the plates. Although both of them implied the feasibility of altering the heat transfer rate by tweaking the flow field, their work focused on the perspective of general convection problems. Furthermore, all the above numerical studies were based on the computational fluid dynamics (CFD) method with the Navier-Stokes equation. In the last two decades, the lattice Boltzmann

method (LBM) has shown some advantages in solving hydrodynamic problems over the traditional CFD method (Qian *et al.*, 1992; He and Luo, 1997; Succi, 2001) due to its mesoscopic nature, intrinsic parallelism, and intuitive boundary treatment. It has been proved to be especially suitable for cases with complex or special boundaries, and cases considering temperature change and multiphase flow phenomenon (Shan and Chen, 1993; He *et al.*, 1998; Guo *et al.*, 2002a).

This paper presents a 2D model and its LBM solutions of the natural convection behavior of the fluid field in enclosures containing a non-heat-source thin plate. A modified extrapolation scheme for handling the thermal boundary of the thin plate has been proposed and verified, which greatly simplifies the computation without losing key information. We focus more on the contributions by the thin plate to the cooling rate of the fluid contained in the enclosure as well as the overall heat leak reduction through the walls. Affecting factors, such as the compartmental plate position, plate size, and Rayleigh and Nusselt numbers, are analyzed for the coupled flow and temperature fields of the internal convection.

## 2 Model and numerical method

### 2.1 Object description

The geometry and boundary conditions of a representative case model for illustrating the influence of compartmental plate on heat leak are schematically shown in Fig. 1. The 2D computational region is a rectangular space filled with air, cold walls on the top and bottom, and hot walls on the sides. The temperature of the cold wall is fixed at  $T_c$ , which in practical systems is usually created by coolant, such as water or even liquid nitrogen. The thermal boundaries of the hot walls are in the convective condition, which brings a heat flux at any position  $y$ , described by  $q_y = h \times (T_y - T_\infty)$ , into the enclosure. The parameter  $h$  is the convective heat transfer coefficient. The fluid in the enclosure has an initial temperature of  $T_\infty$  and an initial velocity of zero.

The compartmental plates are assumed to be infinitely thin. This assumption not only simplifies the boundary condition of the plate, which will be further elaborated in the next section, but also meets the practical application requirement to keep the introduced heat capacity as low as possible.

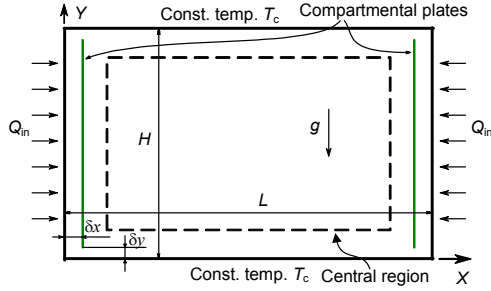


**Fig. 1 Schematic diagram of the physical model and boundary conditions**

$T_c$  is the temperature of the cold wall;  $Q_{in}$  is the heat leak through the hot walls;  $H$  is the height of the enclosure;  $L$  is the length of the enclosure;  $\delta x$  is the distance of plate to the hot wall;  $\delta y$  is the distance of plate edge to the cold wall

To provide a general discussion without making the results restricted to this special case, all physical quantities are converted to dimensionless forms. Specifically, the length/coordinate  $l$ , time  $t$ , and temperature  $T$  are converted as follows:

$$l_d = l / H, \quad (1)$$

$$t_d = t / (1000\delta t), \quad (2)$$

$$T_d = (T - T_c) / (T_\infty - T_c), \quad (3)$$

where  $H$  is the height of the enclosure,  $\delta t$  is the time increment of a single iteration in the LBM model,  $T_\infty$  is the ambient temperature, and  $T_c$  is the temperature of the cold wall. The geometry of the enclosure is considered fixed with an aspect ratio  $L/H$  of 2.

The plates are placed parallel to the  $Y$  axis with a dimensionless distance 0.1 to each of the closest side walls. In application, the region of interest, or the operating space, is the ‘‘central region’’ marked by the dashed rectangle in Fig. 1, instead of the complete computational area. The boundary of the central region is defined as 15% of the total boundary length from one side wall to the other, which means the dimensionless distances to the left and the top walls are 0.3 and 0.15, respectively. In the following discussion, all the mentioned temperature fields focus only on this central region.

The physical properties of the fluid are assumed to satisfy the Boussinesq approximation, which states that all properties are constant except the buoyancy force caused by small variations of density. The buoyancy force is treated as proportional to the tem-

perature difference,  $F = \rho g \alpha_v (T - T_0)$ , where  $\rho$  is the fluid density,  $g$  is the acceleration due to gravity, and  $\alpha_v$  is the volumetric expansion coefficient. The Prandtl number for air at room temperature equals 0.71, which is adopted by many previous studies. The Rayleigh number ( $Ra = g \alpha_v H^3 \Delta T / \nu^2$ , where  $\nu$  is the kinematic viscosity) and the Nusselt number ( $Nu = hH/k$ , where  $k$  is the thermal conductivity) are supposed to be fixed at  $2.62 \times 10^6$  and 15.4, respectively, assuming  $\Delta T = 20$  K and  $h = 8.0$  W/(m<sup>2</sup>·K). Cooling rate and temperature uniformity inside the central region were chosen as the two primary criteria to evaluate the influence of the addition of the compartmental plate.

## 2.2 Numerical method

Thermal LBM was adopted to predict the natural convection behavior in the present model. LBM has been found to be an efficient tool for solving natural convection (Bararnia *et al.*, 2011; Kefayati, 2016; Ren and Chan, 2016) and mixed convection (Kefayati *et al.*, 2012; Bettaibi *et al.*, 2015). Unlike conventional numerical methods based upon the Navier-Stokes equation, the LBM uses pseudo particles that represent information of the distribution function to simulate the flow field.

To apply this method to our case, the computational regime is meshed with uniform grid. On each grid point, two sets of distribution functions are used to describe the flow and temperature field, respectively (Guo *et al.*, 2002a). The temporal evolution of the convection process is represented by a series of time-marching iterations, in which the distribution functions of the pseudo particles undergo a collision process and propagation process, described as the following evolution equations:

$$f_i(\mathbf{x} + \mathbf{c}_i \delta t, t + \delta t) = f_i(\mathbf{x}, t) - \frac{1}{\tau} (f_i - f_i^{eq}) + F_i, \quad (4)$$

$$g_i(\mathbf{x} + \mathbf{c}_i \delta t, t + \delta t) = g_i(\mathbf{x}, t) - \frac{1}{\tau} (g_i - g_i^{eq}), \quad (5)$$

where  $\mathbf{c}_i$  is the discrete velocity in LBM,  $f_i$  is the distribution function for flow field,  $f_i^{eq}$  is the local equilibrium  $f_i$ ,  $F_i$  is the force term in LBM,  $g_i$  is the distribution function for temperature field, and  $g_i^{eq}$  is the local equilibrium  $g_i$ .

The temperature field affects the flow field through buoyancy force, which is implemented by the force term  $F_i$  in Eq. (4). The equilibrium distribution functions and the force term are related to the macroscopic properties, defined as

$$f_i^{eq} = \begin{cases} -\frac{5}{3}p + s_i(\mathbf{u}), & i = 0, \\ \frac{1}{3}p + s_i(\mathbf{u}), & i = 1, 2, 3, 4, \\ \frac{1}{12}p + s_i(\mathbf{u}), & i = 5, 6, 7, 8, \end{cases} \quad (6)$$

$$g_i^{eq} = \frac{T}{4}[1 + 2(\mathbf{c}_i \cdot \mathbf{u})], \quad (7)$$

$$s_i(\mathbf{u}) = \omega_i[3(\mathbf{c}_i \cdot \mathbf{u}) + 4.5(\mathbf{c}_i \cdot \mathbf{u})^2 - 1.5\mathbf{u} \cdot \mathbf{u}], \quad (8)$$

$$F_i = \begin{cases} -\frac{\mathbf{c}_i \cdot \mathbf{g}}{2} \alpha_v (T - T_0), & i = 2, 4, \\ 0, & i = 1, 3, \end{cases} \quad (9)$$

where  $s_i(\mathbf{u})$  is the intermediate function in LBM,  $p$  is the pressure,  $\mathbf{u}$  is the velocity vector, and  $\omega_i$  is the weight coefficient.

After the collide-propagation step, the macroscopic properties can be obtained through the moments of distribution functions,

$$\mathbf{u} = \sum_{i=1}^8 \mathbf{c}_i f_i, \quad p = \frac{c^2}{\sigma} \left[ \sum_{i=1}^8 f_i + s_0(\mathbf{u}) \right], \quad T = \sum_{i=1}^4 g_i. \quad (10)$$

Through a multi-scaling expansion, it was proved that the thermal LBM model using the above evolution steps is numerically equivalent to the incompressible Navier-Stokes equation and energy equation with second-order accuracy (Guo *et al.*, 2002a). Our LBM algorithm is implemented in Python code.

### 2.3 Thermal boundary treatment for the thin plate

As stated earlier, the compartmental plate should be as thin as possible to avoid bringing in additional thermal load due to its own heat capacity. In other words, the plate only serves as a fluid flow blocker and the thermal resistance in the normal direction of the plane is approximately zero. This assumption works well for thin metal plates or foil materials. The

interface between the plate and the fluid is conventionally treated as thermally coupled, which means the heat flux through the interface on each side should be identical. It becomes a tricky problem when the plate is very thin, as the mesh size near the plate is limited by the thickness of the plate, which usually leads to a very large mesh and also brings unnecessary computational costs.

The lattice Boltzmann evolution Eqs. (4) and (5) depicts the iterative solution of the distribution functions for internal nodes, but some  $f_i$  on the boundaries cannot be obtained through collide-propagation, for example,  $f_3, f_6,$  and  $f_7$  for node B1 in Fig. 2. In (Guo *et al.*, 2002b), the unknown distribution functions of boundary nodes are decomposed into equilibrium and non-equilibrium parts, and the unknown macroscopic properties are inherited from the neighboring nodes. Thus, the unknown distribution functions are given by  $f_i = f_i^{eq} + (f_i)_{NN} - (f_i^{eq})_{NN}$ , where the subscript “NN” means neighboring node. Normally, the given boundary condition such as velocity or temperature is applied in the  $f_i^{eq}$  term. However, for our case, as shown in Fig. 2, the two sides of the plate are thermally coupled, which means the temperatures of the boundary nodes B1 and B2 cannot be directly copied from the corresponding nodes. Taking advantage of the “thin plate” assumption, a modified non-equilibrium extrapolation scheme is proposed here. The key point is how to handle the unknown temperature of the plate nodes. For the case shown in Fig. 2, the temperatures of B1 and B2 can be interpolated from those of F1 and F2, as  $T_{B1} = (3T_{F1} + T_{F2})/4$  and  $T_{B2} = (T_{F1} + 3T_{F2})/4$ , respectively. In this way, the heat flux would naturally be conserved, and therefore the thermal coupling condition is satisfied. Mesh densification is no longer required after implementing this modification.

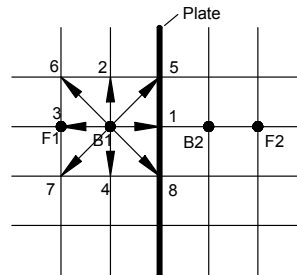


Fig. 2 Modified extrapolation scheme used for the thermal boundary of the thin plate

### 3 Results and discussion

The LBM algorithm is firstly verified upon comparison with reference data from literature, and also with results generated from a traditional Navier-Stokes solver for the same specified conditions. The overall influence of the plate is then evaluated from perspectives of both a transient process and a thermally steady state by optimizing the plate position, size, etc. The Rayleigh and Nusselt numbers are examined to analyze the effects from intrinsic system properties and from the surrounding environment, respectively.

#### 3.1 Model verification

##### 3.1.1 Verification of the LBM algorithm

The coupled fields of flow and temperature were numerically computed by the thermal lattice Boltzmann model with the above boundary treatment scheme. To verify the Python code, we have reproduced the case of a differentially heated cavity (Hortmann *et al.*, 1990; Guo *et al.*, 2002a). The square-shaped cavity is full of air, with its left wall kept at a higher temperature, the right wall kept at a lower temperature, and the top and bottom walls adiabatic. Comparison of the results by this implementation with those in literature is listed in Table 1. The numbers of this work are directly extracted from nodal values without any interpolation. Even so, they match the reference values well.

Further, both a Navier-Stokes solver and the LBM code were applied on the model in Fig. 1 but without a plate inside. The simulation results confirmed that these two methods agree well with each other by inspecting the temperature profiles along several representative characteristic lines, which cover the near boundary region as well as the central region.

The grid size used here is  $201 \times 101$  (nodes). To check the mesh sensitivity, a case four times larger with a grid size of  $401 \times 201$  was also computed. The

average temperature in the central region  $T_{avg}$  and the total heat flux from the side walls were calculated, resulting in a difference of 0.53% and 1.3%, respectively. It can be concluded that  $201 \times 101$  is a reasonable configuration in a compromise between accuracy and computational cost.

##### 3.1.2 Verification of the plate boundary treatment

Verifying the modified non-equilibrium extrapolation scheme is necessary for cases with thin plates added in. To check whether the scheme is equivalent to the coupled conduction-convection method with plate thickness approaching zero or not, we compared the results by the LBM zero-thickness scheme to some traditional coupled schemes with finite thickness.

First, a group of cases with the exact same geometric dimensions, except the plate width, were created and computed using a Navier-Stokes solver. The thermal boundary for the interface between plate (solid) and air (fluid) was set to be coupled, which guarantees the total heat flux through the boundary to be zero. By holding all other parameters steady and adjusting the thickness of the plate, a varying pattern of the temperature field can be obtained. Temperature profiles on the typical characteristic line ( $x=0.2$ ) for the six sets of testing cases with different plate thickness are demonstrated in Fig. 3. A characteristic line is defined as one close enough to the plate but not too close to be influenced by numerical errors. The plate thickness ranges from 0.05 to 0.005 (dimensionless value) in the cases based on Navier-Stokes equation. The LBM results implementing the modified extrapolation scheme are plotted as well, which represents the infinitely small thickness. Fig. 3 shows that at any position in the region of  $y=0.2-0.8$ , the temperature gets lower as  $\delta_{plate}$  decreases, while a reverse trend is observed at  $y>0.9$ . However, in both segments the Navier-Stokes curves are getting closer to the LBM curve when the thickness  $\delta_{plate}$  is approaching zero. These results indicate the validity of

**Table 1** Verification of the thermal LBM algorithm with a differentially heated cavity case ( $Ra=1 \times 10^5$ )

Reference	$U_{max}$	$Y_{max}$	$V_{max}$	$X_{max}$	$Nu_{max}$	$yNu$	$Nu_{ave}$
Guo <i>et al.</i> (2002a)	34.6401	0.8547	68.3811	0.0664	7.8229	0.9258	4.5411
Hortmann <i>et al.</i> (1990)	34.7399	0.8558	68.6396	0.0657	7.7201	0.9180	4.5216
Present work	34.8373	0.8550	68.5231	0.0650	7.7570	0.9200	4.5056

Note: variable definitions can be found in (Guo *et al.*, 2002a)

the modified non-equilibrium extrapolation scheme for the treatment of a thermally coupled thin plate with zero thickness.

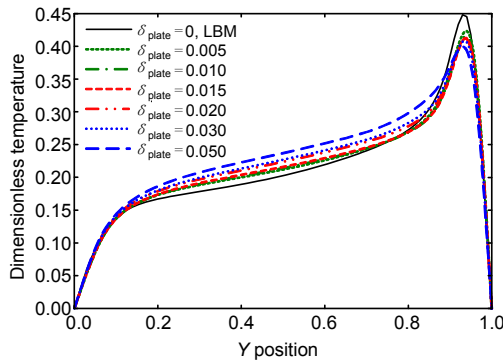


**Fig. 3** Proposed thermal boundary scheme versus CFD results for different plate thickness, all lines correspond to the temperature profile along line  $x=0.2$

### 3.2 Overall influence with addition of the plate

With the help of the efficient LBM code, a comparative study on the overall influence by the compartmental plate at both transient and steady states is presented. To simplify the language, “case N” and “case P” are used in the following part to represent the cases without plates and with plates added, respectively.

#### 3.2.1 Transient performance

The initial state of the system is assumed to be in equilibrium with the environment at a uniform temperature of  $T_\infty$ . As cooling power is delivered through the cold wall, the temperature difference creates density imbalance, and then natural convection of air. During the early stage of the cooling down process, cold waves are generated periodically from the top wall. The magnitude of the wave decays with time when the cold and hot fluids are mixed. Due to this thermal fluctuation, monitoring the transient variance at a single location point is of little value because it may contain much irrelevant random noise. Therefore, a statistical routine is needed for the variables in the central region.

A lumped parameter model using  $T_{\text{avg}}(t)$  was adopted to describe the temporal variance of the system. The mathematical expression of  $T_{\text{avg}}(t)$  can be written as  $T_{\text{avg}}=a_1e^{-a_2t}+a_3$ , where  $a_1$ ,  $a_2$ , and  $a_3$  are positive constants. For comparison, the average

temperature of the central region of the transient cooling process was calculated and shown in Fig. 4. Apart from some minor fluctuations due to the convection waves, the temperature curves well fit the exponential decay, which indicates the validity of the lumped parameter model for this application. In addition, the figure shows that at any time during the cooling down process, the average temperature of case P is always slightly lower. Since the cooling rate is defined as the temperature drop divided by the time before reaching the target temperature, case P has a larger cooling rate. Defined as the time to reach half of the temperature drop,  $t_{0.5}$  is used to quantify this statement. For the cases N and P,  $t_{0.5}$  is 56 and 53 in dimensionless time units, respectively. That is, case P took 6% less time to reach  $\Delta T/2$ , which is not significant, but indeed noticeable. In addition, it should also be mentioned that case P evolves to an obviously lower equilibrium temperature.

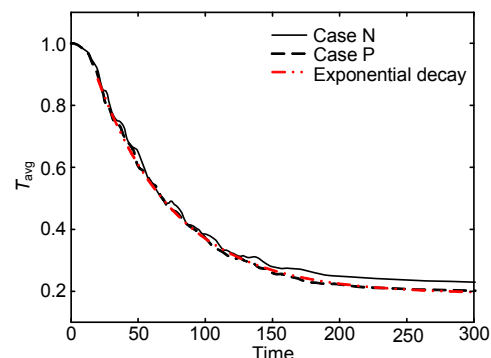


**Fig. 4** Comparison of the transient process for the average temperature of the central region

Another factor of interest is the heat leak through the hot walls, which reflects the varying thermal load of the system. A comparative graph of the heat flux between cases P and N is given as Fig. 5. The two cases are initially fairly close because the thermal influence of the plate has not spread to the hot wall yet. Subsequently, case N shows a much higher average heat flux, since the convective flow is bringing the cold air closer to the hot walls, resulting in a larger temperature difference. As the convective flow develops into steady state, the difference of heat flux between these two cases diminishes to a trivial value (0.795%). Obviously, the curve of case P is much smoother than that of case N, suggesting that the fluctuation caused by convection is effectively

suppressed by the plate installed near the side walls in case P.

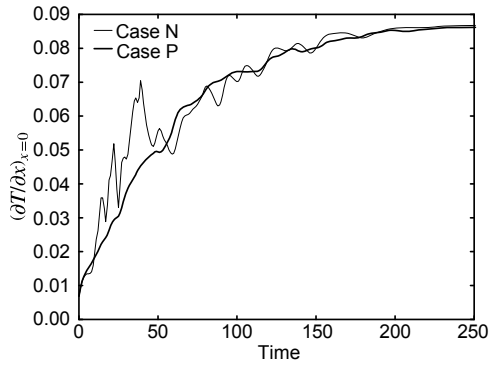


Fig. 5 Comparison of heat flux curve from the hot walls

### 3.2.2 Thermally equilibrium state

The magnitudes of the fluctuation of the velocity and temperature fields decay along time, and tend to reach thermal equilibrium states. In terms of the temperature, as shown in Fig. 6 (plate marked by the blue bar), the addition of the plate leads to an overall lower temperature in the central field, although it also causes a slightly higher temperature near the upper part of the hot walls. Nevertheless, the overall temperature fields of the two cases are alike but with a few isotherm lines shifted in the flow direction. The patterns of temperature field can be better shown, as in Fig. 7, by plotting the temperature curves along characteristic lines. Observations can be characterized in three ways for case P: (a) a slightly higher temperature of the upper region near the side walls, (b) a smaller temperature variation in the central region, and (c) a lower average temperature of the central region.

The behavior of the coupled velocity field should also be taken into account for assessing the contribution by the plate to the cooling rate and temperature uniformity. As shown in Fig. 8, the flow patterns of cases N and P are similar to each other: air is heated near the hot walls, driven up to the top by buoyancy, cooled down by the cold wall, and finally flows back to the bottom. The major difference is that the existence of the plate causes the hot air to concentrate at the top of the gap between the plate and the hot wall, corresponding to the 0–0.1 part of the blue lines in Fig. 7.

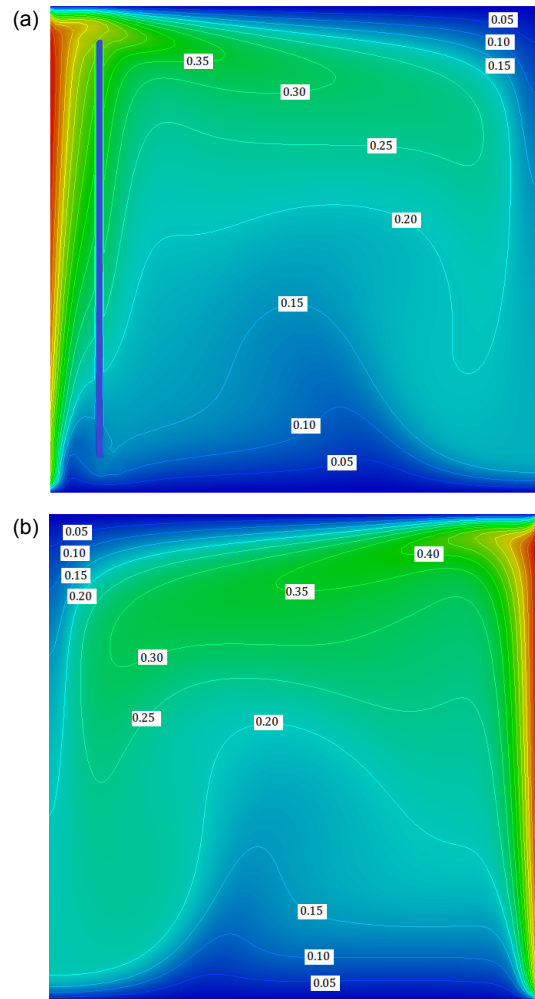


Fig. 6 Comparative view of the temperature field in equilibrium state: (a) case P; (b) case N

Note: for interpretation of the references to color in this figure, the reader is referred to the web version of this article

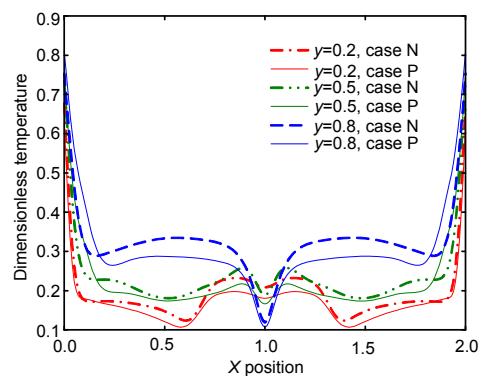
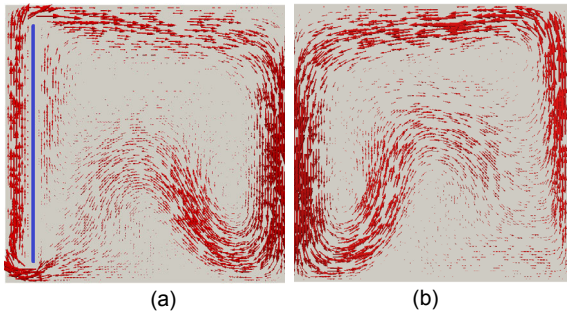


Fig. 7 Comparison of temperature profiles, with plate vs. no plate

Note: for interpretation of the references to color in this figure legend, the reader is referred to the web version of this article



**Fig. 8 Comparison of velocity field with thin plate shield (the vector lengths correspond to velocity magnitude): (a) case P; (b) case N**

The next question is why the average temperature is lower in case P. It should be noticed that the compartmental plate raises the average temperature near the side walls, therefore leading to a lower convection rate with the surroundings. However, as it has already been shown in Fig. 5, the heat fluxes of the two cases at the final steady states are very close, which is insufficient to cause the temperature difference in the central region.

The lower  $T_{\text{avg}}$  in case P could be explained by the effect of “pre-cooling”. Firstly, the heated air is forced to flow through the narrow gap between the plate and the top wall, which is pre-cooled by the cold wall before entering the central region. Secondly, in the bottom part, before the air flows back to the hot walls, the air again has to go through the other gap near the bottom wall, releasing additional thermal energy before being heated once again. This effect also causes a lower temperature at the bottom of the gap between plate and hot wall, which is shown by the blue lines in Fig. 7. The plate has little influence on the total flux through the hot walls at steady state, because the bottom part is already “sub-cooled”, although the upper part of the gap is “over-heated”.

The standard deviation of temperature is used to quantify the temperature variation or uniformity,

$$\sigma_T = \sqrt{\frac{\sum_N (T_i - T_{\text{avg}})^2}{N}}, \quad (11)$$

where  $N$  is the total number of lattice nodes in the central region.  $\sigma_T$  were calculated to be  $7.059 \times 10^{-2}$  and  $5.218 \times 10^{-2}$  (26% smaller) for cases N and P, respectively. The considerably better temperature

uniformity of case P is mainly due to the convective flow partially blocked by the plate. The total heat transfer flux comes from the heat conduction across the temperature gradient and thermal dissipation with mass transfer. The temperature profiles as shown in Fig. 6 are almost identical for both cases, which means the heat flux through conduction is relatively small. However, heat dissipation through the fluid flow is significantly changed by the existence of plates. A major difference in the heat flux by dissipation is indicated by the noticeably smaller overall velocity magnitude in Fig. 8a compared with that of Fig. 8b. With the addition of a compartmental plate, a weaker heat interaction takes place at the border of the central region, breaking the thermal equilibrium, and resulting in a more uniform temperature field.

### 3.3 Plate position and size

#### 3.3.1 Plate position

The position of the compartmental plate (more specifically the distance to the heat-leaking wall) has a substantial influence on the temperature and flow distribution. Fig. 9 shows the average temperature of the central region vs. the distance of the plate to the side wall  $\delta x$ . An interesting behavior is observed that as  $\delta x$  increases, the positive effect of the plate (indicated here by the steady state average temperature) diminishes at first, but starts to enhance after passing a certain position.

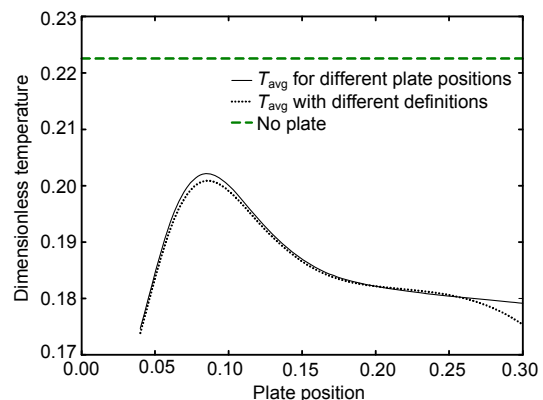


**Fig. 9 Role of plate position (distance to the heat-leaking wall) on the average temperature of the central region**

Analysis of the temperature field near the heat-leaking boundary in Fig. 10 helps to give an intuitive explanation for this behavior. In this figure, for both cases (a) and (b), small  $\delta x$  confines the heat



within the narrow gap between the plate and the wall, and raises the temperature of this region. As  $\delta x$  increases, the flow resistance decreases and takes away more heat from the gas, which lowers the average wall temperature. As a result, a larger amount of heat passing through the wall enters the central region. On the other hand, if the position of the plate is far enough away from the wall, as shown in Figs. 10c and 10d, the convective flow near the wall will be fully developed and less affected by the plate. For this instance, the heat leakage from the side walls is relatively constant. However, as the gap distance increases, the covering area of the cold walls (bottom and top walls) also increases, and provides a stronger pre-cooling effect before the heated air enters the central region.

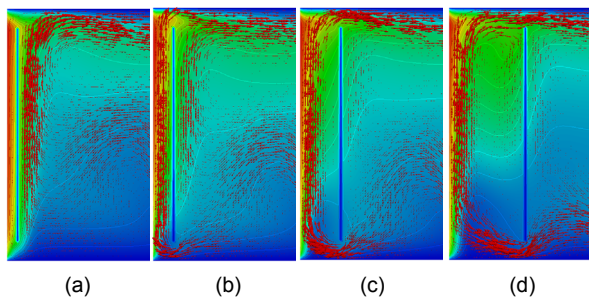


**Fig. 10** Temperature and flow field for different plate positions: (a)  $\delta x=0.004$ ; (b)  $\delta x=0.008$ ; (c)  $\delta x=0.016$ ; (d)  $\delta x=0.030$

Although it is favorable to have the compartmental plate positioned close to the center, practical applications would not normally allow such a design due to the requirement of adequate operation space. Therefore, a more rational and effective choice is to place the compartmental plate as close to the wall as possible, while avoiding contact with the wall.

### 3.3.2 Plate size

Size of the plates is another important aspect that should be considered. As shown by the flow field (Fig. 8a) and temperature field (Fig. 6a), the compartmental plate mainly serves as a blocker to the flow, allowing only a small stream of heated air to get into the central region. Thus, one would naturally expect that a larger plate size is probably helpful in strengthening the positive effect. The results in Fig. 11 confirm this conjecture. The best case takes place when the plate completely covers the side wall.

On the other hand, the contribution of the plate is almost negligible when the relative plate size is smaller than 0.7, because it provides little blockage to the flow through that area (Fig. 8b).

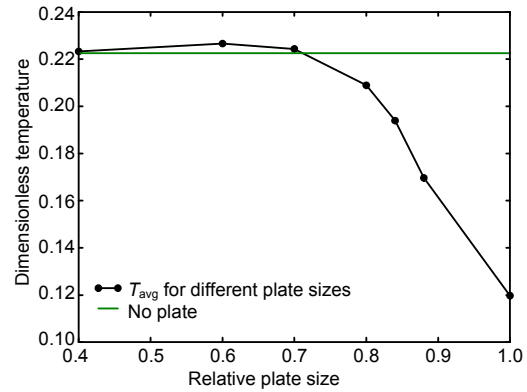


**Fig. 11** Role of plate size on the average temperature of the central region

Fig. 11 also shows that if a relative size of only 0.88 is covered by the plate, an optimal performance improvement (in terms of  $T_{avg}$ ) of 50% can be achieved with much less effort, in comparison to the case with a plate size of 1.0. In general, this suggests that adding a compartmental plate with moderate coverage is a low cost, but effective way to suppress the heat leak.

### 3.4 Effects of $Ra$ and $Nu$

All the above results are calculated with the specified parameters given in Table 1. Further consideration of varying heat leak rate and fluid property are also investigated. The Rayleigh number  $Ra$  and Nusselt number  $Nu$  were chosen as the control variables.  $Nu$  is a measure of the relative heat leak rate.  $Ra$  is a measure of the intrinsic natural property of the system, excluding the heat leak. Therefore,  $Ra$  and  $Nu$  together represent the interior and exterior conditions of the considered problem.

Fig. 12 reveals the relationship between  $T_{avg}$  and the Rayleigh number, as well as the Nusselt number. The value of  $T_{avg}$  varies from 0.178 to 0.197, with  $Ra$  in the range of  $9.5 \times 10^4 - 1.89 \times 10^6$ . Higher Rayleigh number simulations were also conducted. It was found that at  $Ra=3.78 \times 10^6$ , the fluctuation develops into periodic flow instead of diminishing. At  $Ra=7.56 \times 10^6$ , the fluctuation is further reinforced, and turns into turbulent flow. Such a behavior was previously observed (Janssen *et al.*, 1993). In Fig. 12a, as

$Nu$  increases, the temperature difference between cases P and N also increases. It suggests that the addition of the compartmental plate is more beneficial for cases with a larger heat leak rate. On the other hand, Fig. 12b indicates that the effect of the plate is more significant in a low  $Ra$  range.

Fig. 13 presents a comparative view of the steady flow field with different Nusselt and Rayleigh numbers, where all vectors are scaled with the same factor. Figs. 13a–13c show that the Nusselt number has little effect on the distribution of streamlines. It mainly affects the flow intensity, where a larger Nusselt number corresponds to a stronger convective flow. Meanwhile, the Rayleigh number has a stronger

effect on the distribution of the mass flow, despite its relatively weak impact on the temperature field as shown in Fig. 12. For a larger Rayleigh number, the flow tends to merge into a “main stream”, forming clearer macro vortexes, while for a smaller Rayleigh number, the flow is more uniformly distributed, and only two vortexes are formed (no third one at the bottom left).

## 4 Conclusions

Numerical modeling confirms that adding thin compartmental plates close to the heat-leaking walls

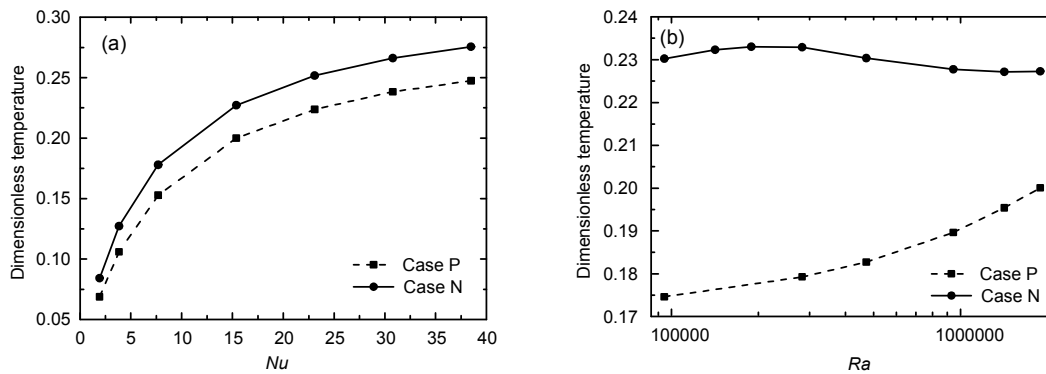


Fig. 12 Effects of Nusselt number (a) and Rayleigh number (b) on the average temperature

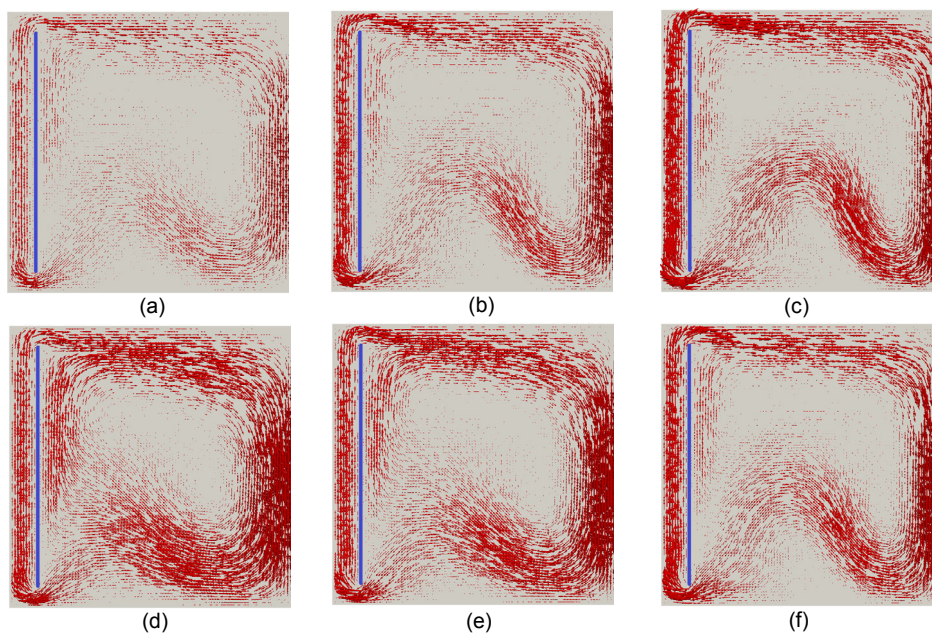


Fig. 13 Variation of flow field with different Nusselt numbers (a)–(c) and Rayleigh numbers (d)–(f). All vectors are zoomed to the same scale

(a)  $Nu=3.85$ ; (b)  $Nu=15.79$ ; (c)  $Nu=38.48$ ; (d)  $Ra=9.45 \times 10^4$ ; (e)  $Ra=4.72 \times 10^5$ ; (f)  $Ra=1.42 \times 10^6$

is an assistive measure to diminish the negative effects of heat leak. Comparative cases with and without plates installed were investigated for both transient processes and steady state performances. The analysis on the transient process showed that the cool down process followed an exponential decay behavior by the lumped model. The insertion of thin plates leads to a higher average cool down rate. It saves 6% of the time to reach the halfway point of the cooling process to the steady state. At the steady state, positive effects of the plate are also observed, such as a lower thermally equilibrium temperature and better temperature uniformity. The thin plate has little negative effect on the total thermal load; however, it alters the flow field, and thus helps reducing the amount of heat entering the central region.

The geometrical factors, including the plate's position and size, are considered. For all the considered cases, with plates positioned at around 0.09, the equilibrium temperature was significantly lowered. From a practical perspective, the suggested placement of the plate is as close to the heat-leaking wall as possible, but not contacting. A larger plate generates a more favorable performance, which means ideally, the plate should completely cover the heat-leaking wall. However, 90% coverage by the plate will still keep 50% of the benefit.

Analyses from the perspective of the Rayleigh number and the Nusselt number were carried out as indicators of the intrinsic property of the system and of the environmental influence, respectively.  $Nu$  affects the near-wall flow, but barely changes the overall flow pattern, while  $Ra$  is closely related to the bulk convection. The beneficial effects of adding the compartmental plate is found to be enhanced at larger  $Nu$  or smaller  $Ra$ .

## References

- Altaç, Z., Kurtul, Ö., 2007. Natural convection in tilted rectangular enclosures with a vertically situated hot plate inside. *Applied Thermal Engineering*, **27**(11-12):1832-1840.  
<http://dx.doi.org/10.1016/j.applthermaleng.2007.01.006>
- Bararnia, H., Soleimani, S., Ganji, D.D., 2011. Lattice Boltzmann simulation of natural convection around a horizontal elliptic cylinder inside a square enclosure. *International Communications in Heat and Mass Transfer*, **38**(10):1436-1442.  
<http://dx.doi.org/10.1016/j.icheatmasstransfer.2011.07.012>
- Ben-Nakhi, A., Chamkha, A.J., 2007. Conjugate natural convection in a square enclosure with inclined thin fin of arbitrary length. *International Journal of Thermal Sciences*, **46**(5):467-478.  
<http://dx.doi.org/10.1016/j.ijthermalsci.2006.07.008>
- Bettaibi, S., Sediki, E., Kuznik, F., et al., 2015. Lattice Boltzmann simulation of mixed convection heat transfer in a driven cavity with non-uniform heating of the bottom wall. *Communications in Theoretical Physics*, **63**(1): 91-100.  
<http://dx.doi.org/10.1088/0253-6102/63/1/15>
- Bilgen, E., 2005. Natural convection in cavities with a thin fin on the hot wall. *International Journal of Heat and Mass Transfer*, **48**(17):3493-3505.  
<http://dx.doi.org/10.1016/j.ijheatmasstransfer.2005.03.016>
- Corvaro, F., Paroncini, M., 2009. An experimental study of natural convection in a differentially heated cavity through a 2D-PIV system. *International Journal of Heat and Mass Transfer*, **52**(1-2):355-365.  
<http://dx.doi.org/10.1016/j.ijheatmasstransfer.2008.05.039>
- Costa, V.A.F., 2012. Natural convection in partially divided square enclosures: effects of thermal boundary conditions and thermal conductivity of the partitions. *International Journal of Heat and Mass Transfer*, **55**(25-26):7812-7822.  
<http://dx.doi.org/10.1016/j.ijheatmasstransfer.2012.08.004>
- Frederick, R.L., 2007. Heat transfer enhancement in cubical enclosures with vertical fins. *Applied Thermal Engineering*, **27**(8-9):1585-1592.  
<http://dx.doi.org/10.1016/j.applthermaleng.2006.09.009>
- Guo, Z., Shi, B., Zheng, C., 2002a. A coupled lattice BGK model for the Boussinesq equations. *International Journal for Numerical Methods in Fluids*, **39**(4):325-342.  
<http://dx.doi.org/10.1002/flid.337>
- Guo, Z., Zheng, C., Shi, B., 2002b. An extrapolation method for boundary conditions in lattice Boltzmann method. *Physics of Fluids*, **14**(6):2007-2010.  
<http://dx.doi.org/10.1063/1.1471914>
- He, X., Luo, L.S., 1997. Theory of the lattice Boltzmann method: from the Boltzmann equation to the lattice Boltzmann equation. *Physical Review E*, **56**(6): 6811-6817.  
<http://dx.doi.org/10.1103/PhysRevE.56.6811>
- He, X., Chen, S., Doolen, G.D., 1998. A novel thermal model for the lattice Boltzmann method in incompressible limit. *Journal of Computational Physics*, **146**(1):282-300.  
<http://dx.doi.org/10.1006/jcph.1998.6057>
- Hortmann, M., Perić, M., Scheuerer, G., 1990. Finite volume multigrid prediction of laminar natural convection: bench-mark solutions. *International Journal for Numerical Methods in Fluids*, **11**(2):189-207.  
<http://dx.doi.org/10.1002/flid.1650110206>
- Jami, M., Mezrhab, A., Bouzidi, M., et al., 2006. Lattice-Boltzmann computation of natural convection in a partitioned enclosure with inclined partitions attached to its hot wall. *Physical A: Statistical Mechanics and Its Applications*, **368**(2):481-494.  
<http://dx.doi.org/10.1016/j.physa.2005.12.029>
- Janssen, R.J.A., Henkes, R.A.W.M., Hoogendoorn, C.J., 1993.

- Transition to time-periodicity of a natural-convection flow in a 3D differentially heated cavity. *International Journal of Heat and Mass Transfer*, **36**(11):2927-2940. [http://dx.doi.org/10.1016/0017-9310\(93\)90111-I](http://dx.doi.org/10.1016/0017-9310(93)90111-I)
- Kefayati, G.R., 2016. Simulation of heat transfer and entropy generation of MHD natural convection of non-Newtonian nanofluid in an enclosure. *International Journal of Heat and Mass Transfer*, **92**:1066-1089. <http://dx.doi.org/10.1016/j.ijheatmasstransfer.2015.09.078>
- Kefayati, G.R., Gorji-Bandpy, M., Sajjadi, H., et al., 2012. Lattice Boltzmann simulation of MHD mixed convection in a lid-driven square cavity with linearly heated wall. *Scientia Iranica*, **19**(4):1053-1065. <http://dx.doi.org/10.1016/j.scient.2012.06.015>
- Ling, C.M., Wang, Q.W., Tao, W.Q., et al., 1999. Experimental study on transient natural convection in a cube enclosure with an isolated vertical cyclically heated plate. *Journal of Thermal Science*, **8**(1):51-58. <http://dx.doi.org/10.1007/s11630-999-0024-6>
- Qian, Y.H., D'Humières, D., Lallemand, P., 1992. Lattice BGK models for Navier-Stokes equation. *EPL (Europhysics Letters)*, **17**(6):479-484. <http://dx.doi.org/10.1209/0295-5075/17/6/001>
- Ren, Q., Chan, C.L., 2016. Natural convection with an array of solid obstacles in an enclosure by lattice Boltzmann method on a CUDA computation platform. *International Journal of Heat and Mass Transfer*, **93**:273-285. <http://dx.doi.org/10.1016/j.ijheatmasstransfer.2015.09.059>
- Shan, X., Chen, H., 1993. Lattice Boltzmann model for simulating flows with multiple phases and components. *Physical Review E*, **47**(3):1815-1819. <http://dx.doi.org/10.1103/PhysRevE.47.1815>
- Succi, S., 2001. *The Lattice Boltzmann Equation for Fluid Dynamics and beyond*. Oxford University Press, New York.
- Yang, M., Tao, W.Q., 1995. Three-dimensional natural convection in an enclosure with an internal isolated vertical plate. *Journal of Heat Transfer*, **117**(3):619-625. <http://dx.doi.org/10.1115/1.2822622>

## 中文概要

**题目:** 壁面漏热的冷却腔体内增加薄壁隔板引起的热效应数值研究

**目的:** 评估增加薄壁隔板对于降低封闭腔中漏热面的作用, 为在实际系统中采用薄壁隔板提高温度均匀性的可行性提供理论依据。

**创新点:** 提出一种新的非平衡态外推边界处理方法; 提出在封闭冷却墙体内增加薄壁隔板的有效漏热控制方法。

**方法:** 采用热格子波尔兹曼 (Boltzmann) 方法以及针对薄壁隔板的改进型非平衡态热边界条件处理方法, 将数值计算与理论分析相结合, 研究漏热冷却腔体内的动态过程。

**结论:** 1. 在漏热壁面附近增加薄壁隔板可使壁面漏热的冷却箱体内降温时间缩短, 并且最终达到更好的温度均匀性。2. 薄壁隔板的位置靠近漏热面可增强其效果, 隔板尺寸越大效果越好。3. 在更大的努塞尔数 ( $Nu$ ) 或更小的瑞利数 ( $Ra$ ) 条件下, 增加隔板所起到的效果更加明显。

**关键词:** 隔板; 封闭腔; 自然对流; 格子波尔兹曼; 冷却速率; 温度均匀性